AMERICAN SOCIETY FOR MICROBIOLOGY | Microbiology Spectrum

RESEARCH ARTICLE

Commensals Serve as Natural Barriers to Mammalian Cells during *Acanthamoeba castellanii* Invasion

Yu-Jen Wang,[a,b] Chun-Hsien Chen,[a] Jenn-Wei Chen,[a,d] Wei-Chen Lin[a,c,d]

[a]Institute of Basic Medical Sciences, College of Medicine, National Cheng Kung University, Tainan, Taiwan
[b]Department of Clinical Laboratory, Chest Hospital, Ministry of Health and Welfare, Tainan, Taiwan
[c]Department of Parasitology, College of Medicine, National Cheng Kung University, Tainan, Taiwan
[d]Department of Microbiology and Immunology, College of Medicine, National Cheng Kung University, Tainan, Taiwan

ABSTRACT *Acanthamoeba castellanii* is a free-living, pathogenic ameba found in the soil and water. It invades the body through ulcerated skin, the nasal passages, and eyes and can cause blinding keratitis and granulomatous encephalitis. However, the mechanisms underlying the opportunistic pathogenesis of *A. castellanii* remain unclear. In this study, we observed that commensal bacteria significantly reduced the cytotoxicity of the ameba on mammalian cells. This effect occurred in the presence of both Gram-positive and Gram-negative commensals. Additionally, commensals mitigated the disruption of cell junctions. *Ex vivo* experiments on mouse eyeballs further showed that the commensals protected the corneal epithelial layer. Together, these findings indicate that *A. castellanii* is pathogenic to individuals with a dysbiosis of the microbiota at infection sites, further highlighting the role of commensals as a natural barrier during parasite invasion.

IMPORTANCE *Acanthamoeba castellanii*, an opportunistic protozoan widely present in the environment, can cause *Acanthamoeba* keratitis and encephalitis in humans. However, only a few reports describe how the ameba acts as an opportunistic pathogen. Our study showed that the normal microbiota interfered with the cytotoxicity of *Acanthamoeba*, persevered during *Acanthamoeba* invasion, and reduced corneal epithelium peeling in the mouse eyeball model. This suggests that commensals may act as a natural barrier against *Acanthamoeba* invasion. In future, individuals who suffer from *Acanthamoeba* keratitis should be examined for microbiota absence or dysbiosis to reduce the incidence of *Acanthamoeba* infection in clinical settings.

KEYWORDS *Acanthamoeba castellanii*, commensals, mammalian cells, cytotoxicity, opportunistic pathogen

Acanthamoeba castellanii is a free-living ameba found in a wide variety of environments, indicating its ability to survive under adverse conditions. It feeds on bacteria, fungi, and other protists (1, 2). Obligate intracellular pathogens, such as *Legionella* spp., *Mycobacterium avium*, *Rickettsia* spp., *Chlamydia* spp., and giant viruses, can grow within *Acanthamoeba* (3–6). These bacteria adapt to the host environment through gene transfer (7), which, in turn, enhances their evolution and pathogenicity (8, 9). For instance, *Legionella* spp. form a membrane-enclosed microenvironment within *A. castellanii* via fusion with other membrane-bound vesicles (10). *Vibrio cholerae* can escape degradation in the cytoplasm of *A. castellanii* by effectively neutralizing pH changes, digestive enzymes, and the production of reactive oxygen radicals in the ameba (11).

In contrast, bacteria in the human normal microbiota, such as *Staphylococcus aureus* and *Escherichia coli*, can serve as food sources for *Acanthamoeba* cells (12). Before being ingested by *A. castellanii*, bacteria adhere to the ameba's outer membrane. The surface of *A. castellanii* expresses a 130-kDa mannose-binding protein (MBP) that plays a role in food source recognition (13). Using the mannose saturation assay, mannose-selected *Acanthamoeba* cells exhibit a

Editor Kevin R. Theis, Wayne State University

Address correspondence to Wei-Chen Lin, wcnikelin@mail.ncku.edu.tw.

The authors declare no conflict of interest.

Received 6 June 2021
Accepted 2 November 2021
Published 22 December 2021

significant decrease in *E. coli* K-12 uptake (14). Polyclonal serum binding to MBP inhibits the association of *S. aureus*, which suggests that *Acanthamoeba* uses MBP in phagocytosis with *S. aureus* (15). Further, *Acanthamoeba* can ingest foods into phagosomes and has lysosomal enzymes responsible for digestion and nutrient acquisition (16). However, studies of the influence of diverse microbial ingestion on the pathological microenvironment of *A. castellanii* are lacking.

Acanthamoeba trophozoites can invade humans through the eyes, nasal passages, and ulcerated or broken skin. When *Acanthamoeba* cells enter the eyes, they can cause severe *Acanthamoeba* keratitis (AK) (17). When they enter through the respiratory system or a skin wound, they can invade the central nervous system by hematogenous dissemination, causing granulomatous amebic encephalitis (GAE) or skin lesions in individuals with compromised immune systems (18). Recent investigations have shown that the human ocular microbiota mostly comprises coagulase-negative *Staphylococcus*, *Staphylococcus aureus*, and *Escherichia coli* (19–21). *Staphylococcus epidermis*, *S. aureus*, and *E. coli* have been the focus of many studies on colonization resistance in the skin (22, 23). A study of the nasal microbiota in healthy humans demonstrated that *Corynebacterium* and *Staphylococcus* were prevalent in most samples (24). Previous studies have shown that the resident microbiota functions to establish and maintain human immune homeostasis (25, 26). Therefore, upon penetration of *A. castellanii* into the eyes, nasal passage, and skin, the relationship between the ameba and the host microbiota might play a crucial role in the progression of AK and GAE.

In this study, we evaluated interactions between *A. castellanii* and commensals through the cytopathic effect (CPE) assay and recorded the results of a triculture involving *A. castellanii*, *S. aureus*, or *E. coli* and mammalian cells over time. The processes involved in *A. castellanii* pathogenicity were examined. Epithelial cell junction proteins were assessed to investigate the influence of *A. castellanii* on its microenvironment. These results were validated using an *ex vivo* mouse model. Thus, this research will help us better understand the role of normal microbiota and its dysbiosis in AK and GAE progression.

RESULTS

Heat-killed commensals reduced *Acanthamoeba* pathogenicity in C6 cells. To understand the effects of commensals on the pathogenesis of *Acanthamoeba castellanii*, we assessed the CPE on cells by coculturing *A. castellanii* with *Escherichia coli* or *Staphylococcus aureus*. Cell monolayers showed different disruption levels at 3 h postinfection (POI), and heat-killed commensals inhibited the ameba's pathogenesis within 6 h POI (Fig. 1a). We further quantified the cytotoxicity of *A. castellanii* in the presence of commensal coculture using the lactate dehydrogenase (LDH) assay. Coculture of *A. castellanii* with heat-killed and intact *E. coli* reduced its cytotoxicity, but this did not occur with live *E. coli* and bacterial debris (Fig. 1b). *S. aureus*, a Gram-positive bacterium, also showed similar effects on the cytotoxicity of *A. castellanii* in the LDH assay (Fig. 1c). To validate these results, we performed coculture and triculture studies. As shown in Figure 2, *A. castellanii* cells repeatedly crawled over nearby mammalian cells, resulting in cell rounding in coculture. In contrast, *A. castellanii* cells in triculture showed active feeding behavior around heat-killed commensals and ingested them (Fig. 2). These findings suggest that intact commensals might play a crucial role in the ameba's pathogenicity.

The presence of commensals interfered with the phagocytic ability of *Acanthamoeba*. *A. castellanii* pathogenicity occurs via three major mechanisms: adhesion, protein secretion, and phagocytosis. We investigated whether commensals interfered with the ameba's pathogenesis mechanisms. The CPE assay showed that the presence or absence of heat-killed commensals did not inhibit the attachment of *A. castellanii* cells (Fig. 3a). The percentage of attached *A. castellanii* cells was approximately 100% in all groups (Fig. 3b). Furthermore, culture supernatant suspected of having secreted proteins of *A. castellanii*, along with heat-killed commensals, was added to the C6 cells. However, the commensals did not neutralize the cytotoxicity of the secreted proteins (Fig. 3c). We further tested the effect of commensals on the phagocytic ability of *A. castellanii* by comparing the bacterial concentration with *A. castellanii* cytotoxicity and found them to be inversely proportional within 6 h POI. However, at 8 h POI, the concentration of commensals remained constant and *A. castellanii* cytotoxicity

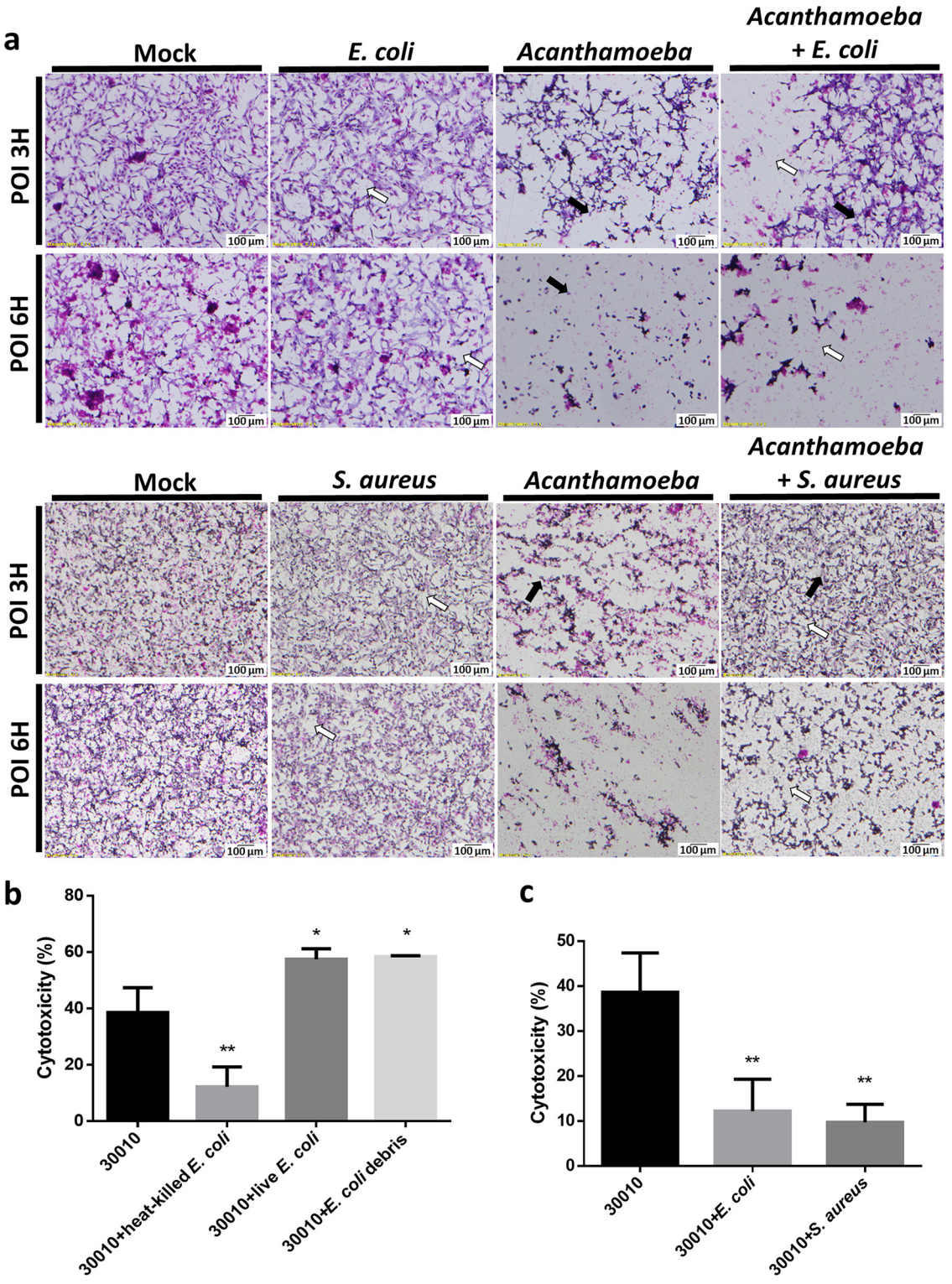

FIG 1 Commensal interference in the cytopathogenicity of *Acanthamoeba castellanii* on C6 cells. (a) Treatment of rat glial C6 cells with *A. castellanii* ATCC-30010 alone (black arrows) or with heat-killed *Escherichia coli* or *Staphylococcus aureus* (white arrows); evaluation of the cytopathic effects (CPE) by Giemsa staining after incubation for 3 and 6 h. (b) Lactate dehydrogenase assay after C6 cells were treated with *A. castellanii* ATCC-30010 alone, heat-killed *E. coli*, live *E. coli*, or *E. coli* debris for 6 h. The data are representative of three independent experiments. (c) Lactate dehydrogenase assay after the treatment of C6 cells with *A. castellanii* ATCC-30010 alone, heat-killed *E. coli*, or heat-killed *Staphylococcus aureus* for 6 h. The data are representative of three independent experiments. *, $P < 0.05$; **, $P < 0.01$, according to Student's *t* test.

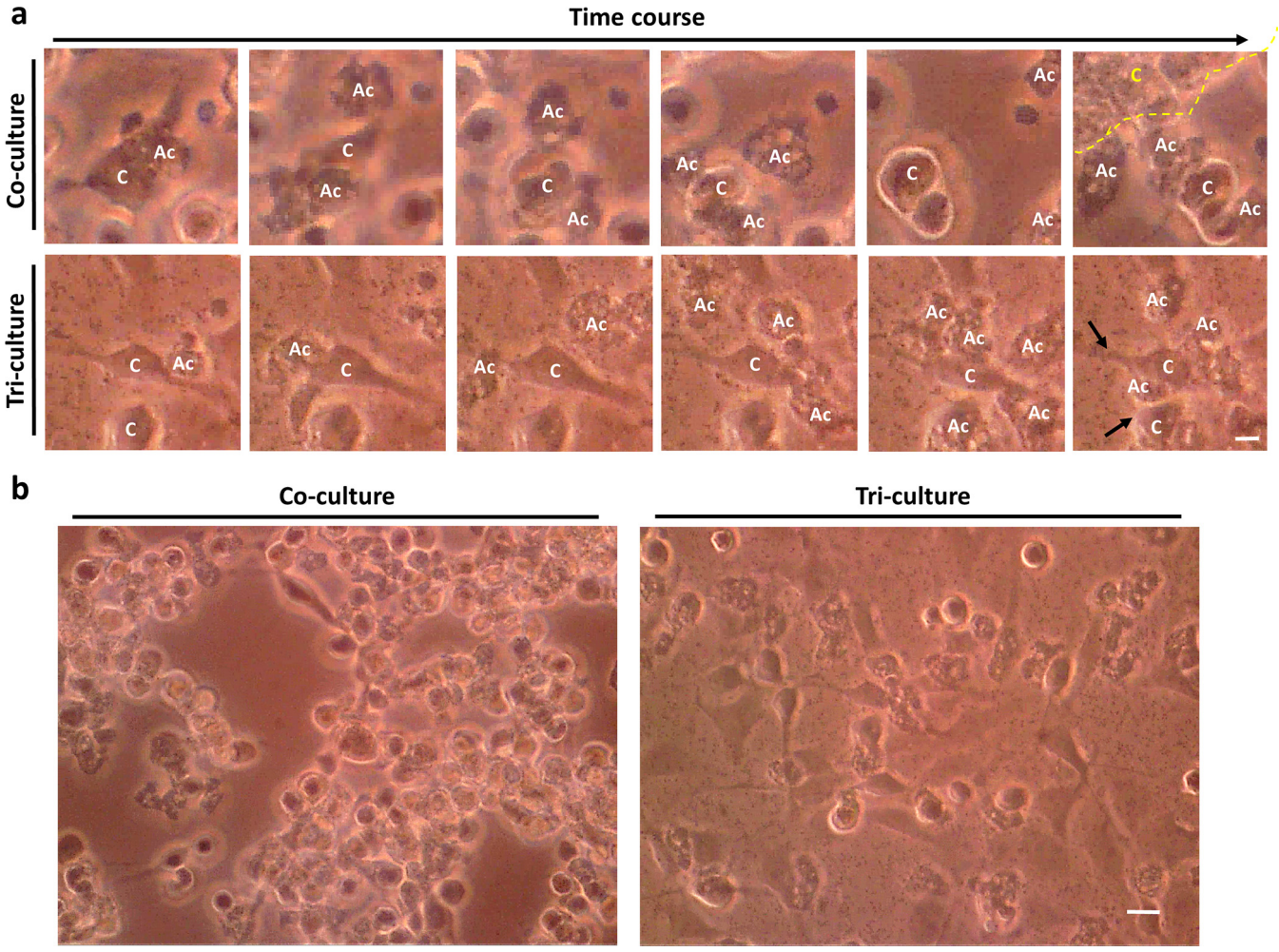

FIG 2 Time course of C6 cells cocultured/tricultured with *Acanthamoeba castellanii* or *A. castellanii* plus *Escherichia coli* within 6 h. (a) Time course micrographs show the cytopathic effects (CPE) of C6 cells induced by being crawled over by *A. castellanii* cells and interference due to bacterial presence. The yellow dotted line encircles clusters of detached cells after *A. castellanii* cells have crawled over them. The black arrows indicate extensive attachment of the cells owing to bacterial presence. C, C6 cells; Ac, *A. castellanii*. (b) Light micrographs showing the CPE of C6 cells after treatment with *A. castellanii* or *A. castellanii* plus *E. coli*. Bar = 25 μm.

was elevated (Fig. 4), which indicated that the presence of commensals interfered with *A. castellanii* phagocytosis, resulting in cytotoxicity reduction.

Preservation of cell junctions by commensals. The disruption of cell junctions is a crucial step for the invasion and ultimately pathogenicity of *A. castellanii*. Western blotting was performed on A549 epithelial cells to screen for the preservation of common cell junctions on epithelial cells, including tight junctions, adherence junctions, desmosomes, and gap junctions. Interestingly, the presence of heat-killed *E. coli* cells significantly reduced the relative expression of epithelial cell junctions, and heat-killed *S. aureus* cells reduced the levels of occludin, junctional adhesion molecule A (JAM-A), and connexin 43 (Fig. 5). This suggests that cell junctions were protected by the presence of commensals, which further prevented the cells from rounding and dying. Thus, the absence of commensals would have led to the breakdown of cell junctions, leading to *A. castellanii* penetration.

The integrity of the corneal epithelium is preserved by commensals during *Acanthamoeba* invasion. The *ex vivo* mouse model was used to test the effect of commensal bacteria on corneal epithelium abrasion by *A. castellanii*. Before infection, the eyeballs of all mice groups had a transparent appearance owing to a preserved corneal epithelium and good refraction. Several scrapes appeared on the ocular surface 24 h POI with *A. castellanii* alone. However, in the group subjected to *A. castellanii* infection along with heat-killed commensals, only a few scrapes were noted (Fig. 6a). A biopsy was performed to evaluate the level

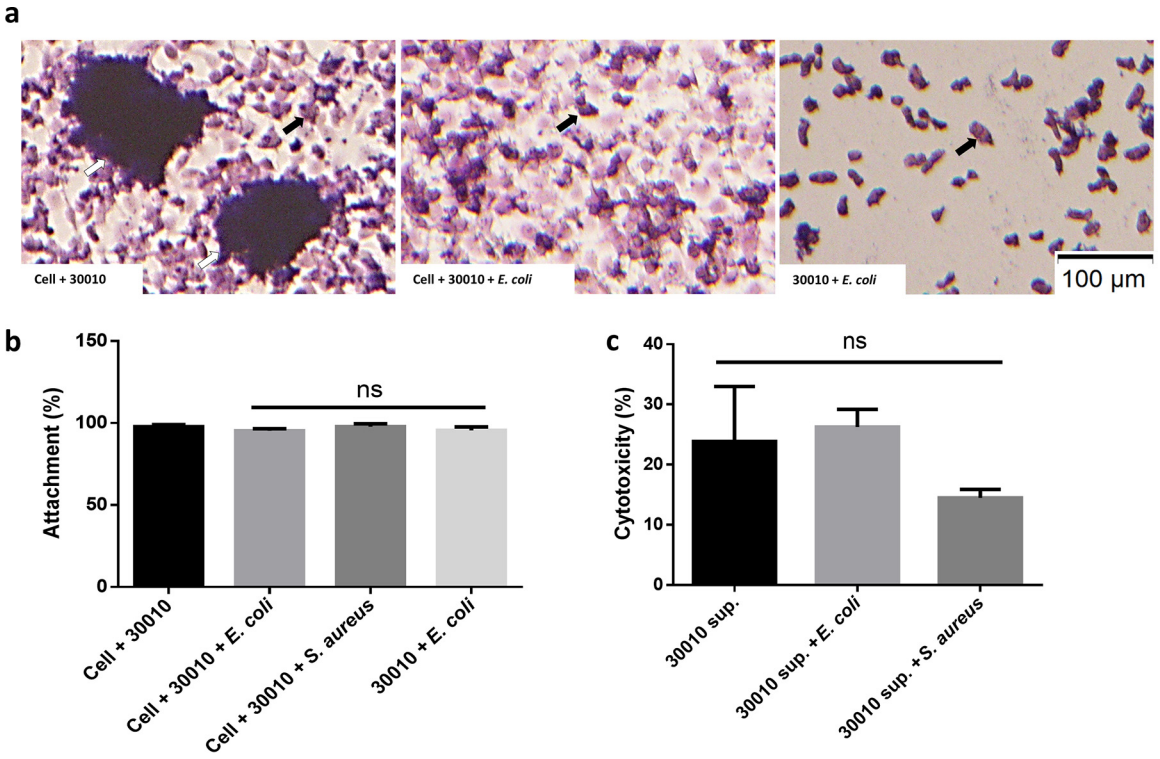

FIG 3 *Acanthamoeba castellanii* cell adhesion and protein secretion ability in the presence of commensals. (a) Images showing *A. castellanii* (black arrows) either attaching to the surface in the presence of bacteria or not. The dead cells were aggregated (white arrows) under *A. castellanii* invasion without bacteria. (b) Attached *A. castellanii* cells were counted after 6 h of coculture/triculture with bacteria or with C6 cells plus bacteria. The data are representative of three independent experiments. (c) Supernatants (sup) containing the proteins secreted by *A. castellanii* cells were added to C6 cells or C6 cells plus commensal bacteria. The data are representative of three independent experiments. ns, not significant according to Student's *t* test, compared to the attachment rate and cytotoxicity.

of cell damage using hematoxylin and eosin (H&E) staining. The outer layer of the corneal epithelium was deeply stained, with a clear boundary, when no infection was present, which was also observable for *A. castellanii* invasion with bacteria. However, for *A. castellanii* infection alone, there was no intact deep-stained corneal epithelium (Fig. 6b). The average corneal thickness of the mouse eyeballs was 11.06 μm. However, the eyeballs treated with *Acanthamoeba* only presented 15.70% corneal epithelium viability and had an average thickness of 1.74 μm. In contrast, the eyeballs with *Acanthamoeba* invasion with bacteria retained 73.16% of the

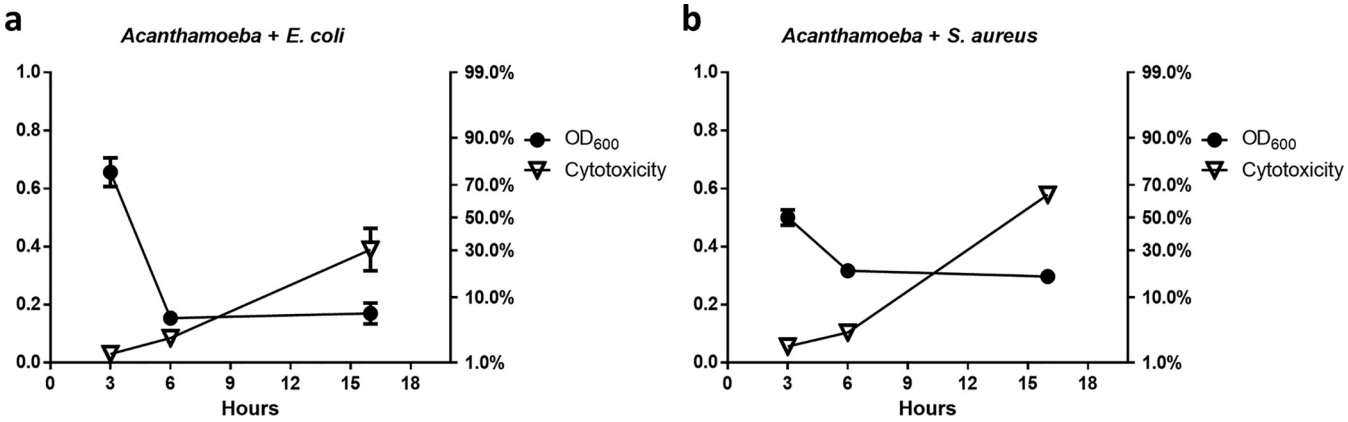

FIG 4 Lactate dehydrogenase assay and measurement of the concentration of heat-killed commensal bacteria to assess their interference in *Acanthamoeba castellanii* phagocytosis. C6 cells were tricultured with *A. castellanii* and an initial concentration at OD_{600} = 0.6 of heat-killed *Escherichia coli* (a) or *Staphylococcus aureus* (b) cells. The lactate dehydrogenase produced by the dead cells and the concentration of the commensals were measured at 3, 6, and 16 h. The data are representative of three independent experiments. The data are expressed as the mean ± standard deviation (SD).

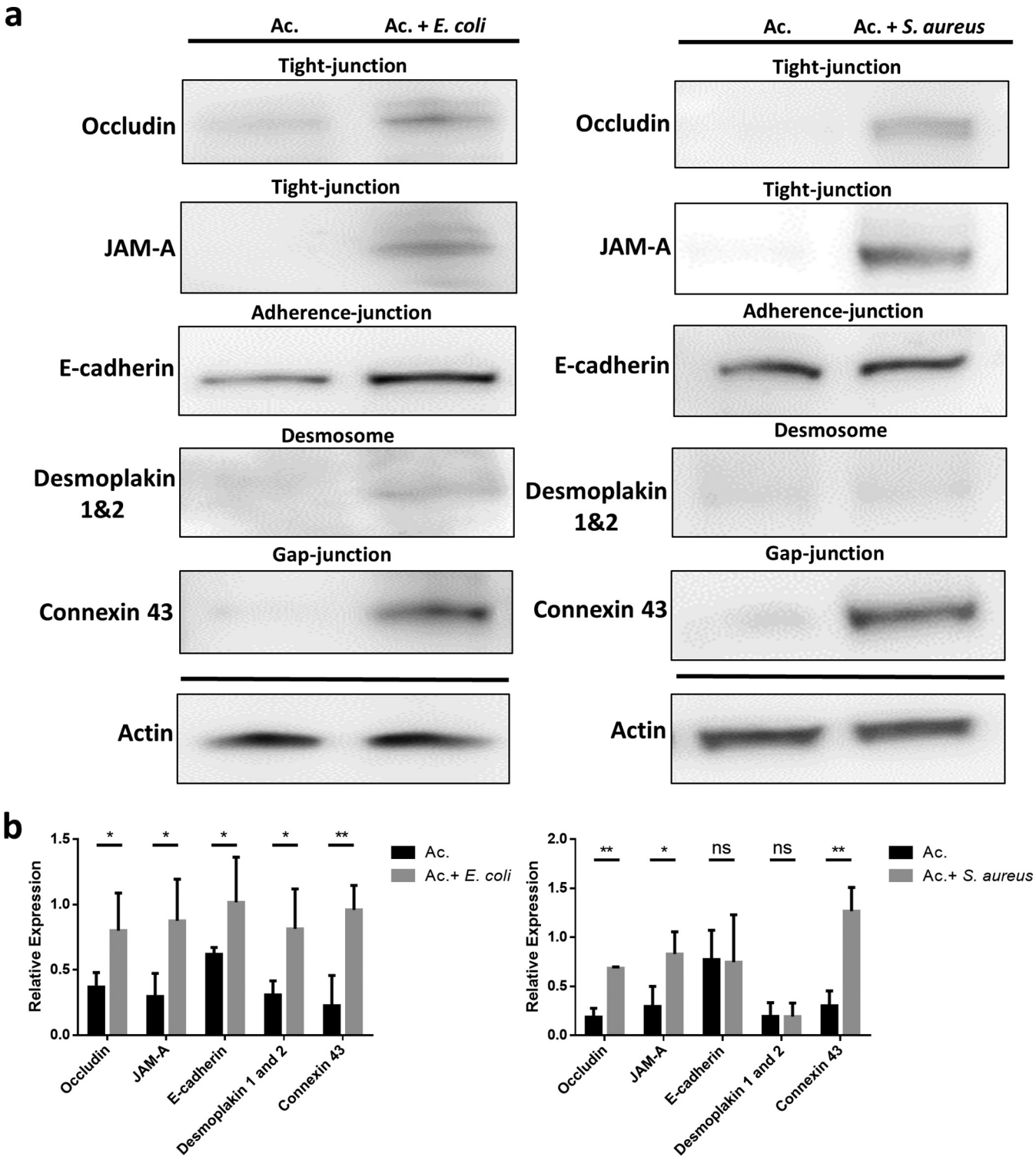

FIG 5 Protection of the cell junctions in the presence of commensals. (a) Sodium dodecyl sulfate-polyacrylamide gel electrophoresis (SDS-PAGE) showing the expression level of tight junction (occludin, JAM-A), adherence junction (E-cadherin), desmosome (desmoplakin 1 and 2), and gap junction (connexin 43) proteins in epithelium A549 coculture/triculture with *Acanthamoeba castellanii* cells alone or with *Escherichia coli* or *Staphylococcus aureus* cells. Examination of the whole-cell extracts by Western blot analysis after 6 h of treatment, with actin used as a loading control. (b) Quantification of the cell junction relative expression level in epithelium A549 coculture/triculture with *A. castellanii* cells alone or with *E. coli* or *S. aureus* cells. The data are representative of three independent experiments, and the protein expression strength was quantified using ImageJ software. *, $P < 0.05$; **, $P < 0.01$; ns, not significant according to Student's *t* test. Ac., *Acanthamoeba*.

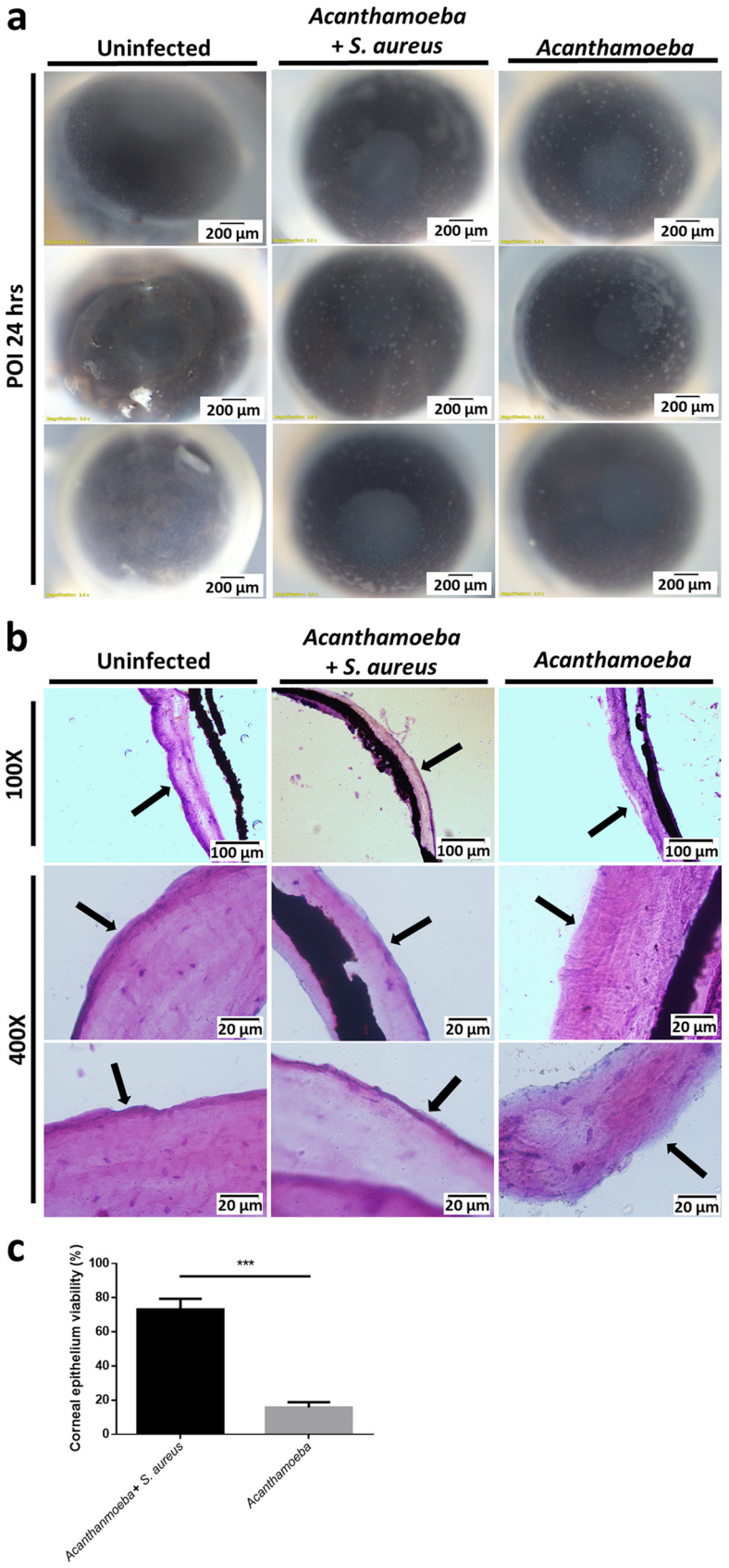

FIG 6 Presence of commensals during *Acanthamoeba castellanii* invasion in the eyeballs of an *ex vivo* mouse model. (a) *Ex vivo* images showing different conditions of the corneal epithelial cells peeling

(Continued on next page)

corneal epithelium viability and had an average thickness of 8.10 μm (Fig. 6c). Thus, the *ex vivo* mouse model provided evidence for the crucial role of commensals in mitigating *A. castellanii* pathogenicity.

DISCUSSION

As a free-living protozoan, *A. castellanii* usually ingests bacteria by directional movement and digests them through phagocytosis (27). A previous study demonstrated that *A. castellanii* pseudopodia contain several receptors that attach to the targets and ingest them (28, 29). However, *A. castellanii* motility decreases under sufficient nutrient conditions (30, 31), suggesting that it can also feed at a fixed position without motility and hunting. Interestingly, our CPE assay and time course capture data were consistent with previous findings (32). The presence of intact commensals significantly reduced *A. castellanii* cytotoxicity. Although *A. castellanii* still crawled on the epithelium, the cell damage was reduced. These data show that if individuals have a healthy microbiota, the incidence of diseases caused by *A. castellanii*, like AK and GAE, will be lower.

A. castellanii uses adhesion as the initial step during the onset of its invasion (33). Proteolytic enzymes and proteases secreted by *A. castellanii*, including cysteine proteases, serine proteases, and metalloproteases (34–36), catalyze the degradation of extracellular peptide bonds (37) and stimulate apoptosis in neuroblastoma cells (38). Additionally, phagocytosis by *A. castellanii* involves the engulfment of host epithelial cell debris and small particles, such as bacteria and yeast (39). Based on this information, we examined the effect of commensals on each step that influenced pathogenesis. Evaluation of *A. castellanii* attachment and secreted proteins indicated that commensals did not affect the cytotoxicity of either factor to mammalian cells. In contrast, a sufficient concentration of commensals significantly reduced the cytotoxicity caused by *A. castellanii* phagocytosis. Furthermore, upon the depletion of commensal bacteria, the cytotoxicity of *A. castellanii* increased. This suggests that commensals obstructed the phagocytic ability of *A. castellanii* during infection.

Junction proteins are molecular components that occupy the space between the contiguous body surface of epithelial cells, which is also important for cell monolayer maintenance (40). However, once the epithelium loses these connections formed by the junction proteins, apoptosis occurs (41). In our study, quantification of the four major epithelial cell junctions showed that commensals protected these cell junctions. The *ex vivo* mouse model showed the same effects of commensal presence during *A. castellanii* infection. H&E staining images showed that peeling of the epithelial layer was prevented in the presence of commensals, which indicates that commensals might serve as a natural barrier to *A. castellanii* infection.

Thus, we found that intact Gram-positive or Gram-negative commensals significantly reduced the phagocytic activity of *A. castellanii* on epithelial cells. In addition, we demonstrated that commensals protected epithelial cell junctions and resulted in cell survival. Finally, we used an *ex vivo* mouse model to validate this effect. Biopsy data showed that the epithelium peeling decreased and a clear epithelial boundary was present in cases where commensals were involved in *A. castellanii* invasion. Future studies should investigate whether probiotic supplementation can protect humans from *A. castellanii* infection and maintain a natural barrier.

MATERIALS AND METHODS

***Acanthamoeba* culture.** The standard strain *Acanthamoeba castellanii* ATCC-30010 was obtained from the ATCC (Manassas, VA, USA). *A. castellanii* strains were cultured in protease peptone-yeast extract-glucose (PYG) medium (20 g peptone, 2 g yeast extract, and 18 g glucose; 1 g sodium citrate dehydrate, 0.98 g $MgSO_4 \times 7H_2O$, 0.355 g $Na_2HPO_4 \times 7H_2O$, 0.34 g KH_2PO_4, and 0.02 g $Fe[NH_4]_2[SO_4]_2 \times 6H_2O$, pH 6.5, in 1,000 mL distilled water

FIG 6 Legend (Continued)
under *A. castellanii* invasion alone or in the presence of commensal bacteria at 24 h postinfection. (b) Biopsy section after hematoxylin and eosin (H&E) staining reveals the cell layer completeness (black arrows) after *A. castellanii* invasion alone or in the presence of commensals. (c) Quantification of the corneal epithelium viability in an *ex vivo* model. The data are representative of three independent experiments. ***, $P < 0.001$, according to Student's *t* test.

and autoclaved at 121°C for 15 min) (42) at 28°C in cell culture flasks and maintained after washing in Page's modified Neff's ameba saline (PAS; 1.2 g NaCl, 0.04 g $MgSO_4$–$7H_2O$, 0.03 g CaCl2, 1.42 g Na_2HPO_4, and 1.36 g KH_2PO_4 in 1 L double-distilled water [ddH_2O]) (43).

Cell culture. Glioma C6 and non-small cell lung cancer cells (A549) were cultured in Dulbecco's minimum essential medium (DMEM) supplemented with 10% fetal bovine serum (FBS) and pen-strep (100 U/mL penicillin and 100 μg/mL streptomycin) (44). Cells were maintained at 37°C and 5% CO_2.

Bacterium processing. *Escherichia coli* strain K-12 and methicillin-resistant *Staphylococcus aureus* cells were used as the ocular microbiota. Heat-killed microbes were subjected to heat shock at 90°C for 5 min, similarly to our previous study (45). To acquire intact microbes, the bacterial debris was collected from live microbes sonicated in DMEM using an ultrasonic probe (BO3 ultrasonic processor UP 1200; Cromtech India). In addition, the optical density (OD) of the processed microbes was adjusted to OD_{600} = 0.5 before supplementation.

Adhesion assays. *A. castellanii* cells were cultured in PYG medium (pH 6.5) at 28°C, and the medium was refreshed 15 to 20 h before the experiments. The trophozoite form of *A. castellanii* was screened by microscopy and collected by placing the flasks on ice for 30 min with gentle agitation. The detached cells were collected by centrifugation at 3,000 rpm for 5 min. Then, they were suspended in 200 ml Page's modified Neff's ameba saline (PAS) and seeded at 1×10^5 amebae/well and incubated with heat-killed *E. coli* strain K-12 or MRSA (OD_{600} = 0.5) for 1 h at 28°C. The unattached amebae were gently collected, added to PAS, and stained with trypan blue for hemocytometer counting. The attachment rate was calculated as follows: ([total amebae – unattached amebae]/total amebae) $\times$ 100 = % attachment (46). All measurements were repeated thrice.

Analysis of neutralization of the secreted proteins. *A. castellanii* strains were seeded into 10-cm culture dishes and cultured in PYG medium (pH 6.5) at 28°C. After reaching confluence, the culture medium was replaced with PAS and cultured for 4 h. The PAS medium from the *A. castellanii* culture was collected and supplied to the cultured C6 cells. Simultaneously, the heat-killed *Escherichia coli* strain K-12 or methicillin-resistant *Staphylococcus aureus* cells were added to the C6 cells along with the medium. Analysis of the neutralization of the secreted proteins and their cytopathic effect was performed after 4 h of coincubation (47).

Cytopathic effect analysis. C6 cells were cultured in 6-well plates (Falcon Plastics; no. 38016), and on attaining confluent monolayers, the medium in the wells was replaced with serum-free 20% DMEM before treatment. *A. castellanii* cells, alone or with heat-killed *E. coli* K-12/MRSA cells, were added to the culture medium and incubated for 6 h. After incubation, the cell monolayers were fixed with 2% paraformaldehyde and stained with Giemsa stain (Merck, Darmstadt, Germany) (48).

Lactate dehydrogenase assay. Cells were grown overnight in 24-well plates to obtain monolayers. These cell monolayers in serum-free 20% DMEM medium were incubated with *A. castellanii* (1×10^5 amebae/well) at 37°C in a 5% CO_2 incubator for 6 h. Cell supernatants were collected, and the cytotoxicity was determined by measuring the LDH release (cytotoxicity detection kit; Roche). The absorbance of the product obtained from the reaction with LDH was measured at 492 nm using a Multiskan SkyHigh microplate spectrophotometer (Thermo Fisher Scientific). For the positive control, 1% Triton X-100 was used on the cell monolayers for 100% cell death. In contrast, untreated cells served as the negative control. The absorbance was converted to cytotoxicity as follows: ([sample value – negative-control value]/[positive-control value – negative-control value]) $\times$ 100 = % cytotoxicity (49). All the determined CPE values were repeated thrice.

Time-course and image capture. Dynamic images of *A. castellanii* invasion were captured using an Olympus microscope (Tokyo, Japan) with a digital camera (AM7025X Edge; Dino-Lite, Taiwan). The capture interval of each image was set at 10 min using DinoCapture version 2.0 (Dino-Lite). To characterize the influence of the commensal bacteria, coculture, and triculture images were captured using an MV PLAPO 2XC dissection microscope (Olympus) after methanol fixation, Giemsa staining, and evaluation of the *ex vivo* mouse model.

Western blotting. A549 cells were cultured in 10-cm petri dishes and grown at 37°C in a 5% CO_2 incubator in DMEM containing FBS. After 24 h, the A549 cell monolayer was tricultured with *A. castellanii* cells (1×10^5 amebae/dish) and heat-killed *S. aureus*/*E. coli* cells for 6 h. The protein lysate was collected after incubation, and the total protein extract was separated by sodium dodecyl sulfate-polyacrylamide gel electrophoresis (SDS-PAGE). The proteins were transferred onto a polyvinylidene fluoride membrane, which was blocked with 3% skimmed milk in phosphate-buffered saline at 25°C, and then incubated overnight with monoclonal antibodies at 4°C. The blots were then incubated with horseradish peroxidase (HRP)-conjugated IgG for 1 h at 25°C. Proteins were detected using Immobilon Western HRP substrate (50). The optical densities of the bands were measured using ImageJ software (51).

Ethics statement. All the animal experimental procedures were reviewed and approved by the Institutional Animal Care and Use Committee (IACUC) of the Laboratory Animal Research Center at National Cheng Kung University (NCKU) (approval NCKU-IACUC-109-015).

***Ex vivo* mouse model.** Because the *in vivo A. castellanii* infection model is unstable to date, we developed an *ex vivo* mouse model modified from a previous study on *Acanthamoeba* infection (52, 53). Briefly, three eyeballs from each group of mice were obtained from sacrificed ~6 to 8-week-old BALB/c mice without ocular disorders. The separated eyeballs were placed with the cornea side up in a 48-well plate containing 20% DMEM for 5% soft agar fixation. *A. castellanii* cells (1×10^5 amebae) with/without heat-killed bacteria (OD_{600} = 0.5) were added to the wells and incubated at 28°C. After 24 h, the appearance of the eyeballs was recorded using a dissection microscope; they were then fixed in 10% formalin for staining with H&E solution (54). Quantification of the corneal epithelium viability was performed using ImageJ software to evaluate the corneal epithelium thickness. Briefly, biopsy specimen images were inverted to a single color. The standard corneal epithelium thickness was adjusted using the

average epithelium thickness of the control eyeballs. Each group of eyeballs treated with *A. castellanii* with/without heat-killed bacteria was measured in the same way as the control eyeballs. The corneal epithelium viability of the cells was calculated as follows: (average thickness of single eyeball/average thickness of control) × 100%. Three independent experiments were conducted.

Statistical analysis. The data were expressed as the mean ± standard deviation (SD). All comparisons were analyzed using unpaired two-tailed Student's *t* tests. Statistical significance was set at $P < 0.05$. The statistical data were calculated and analyzed using GraphPad Prism version 5.0 software (La Jolla, CA, USA).

Data availability. The raw data supporting the conclusions of this article will be made available by the authors upon reasonable request.

ACKNOWLEDGMENTS

We thank Yu-Min Kuo in the Department of Cell Biology and Anatomy College of Medicine at National Cheng Kung University for supporting the technology of mouse eyeball harvesting.

W.-C.L. conceived and designed the study; Y.-J.W., C.-H.C., and W.-C.L. analyzed the data; Y.-J.W. and J.-W.C. wrote the paper. All authors read and approved the final version of the manuscript.

The Ministry of Science and Technology (MOST) provided a grant to W.-C.L. (MOST 109-2628-B-006-022).

REFERENCES

1. Denet E, Coupat-Goutaland B, Nazaret S, Pelandakis M, Favre-Bonte S. 2017. Diversity of free-living amoebae in soils and their associated human opportunistic bacteria. Parasitol Res 116:3151–3162. https://doi.org/10.1007/s00436-017-5632-6.
2. Schulz F, Lagkouvardos I, Wascher F, Aistleitner K, Kostanjšek R, Horn M. 2014. Life in an unusual intracellular niche: a bacterial symbiont infecting the nucleus of amoebae. ISME J 8:1634–1644. https://doi.org/10.1038/ismej.2014.5.
3. Scheid P. 2014. Relevance of free-living amoebae as hosts for phylogenetically diverse microorganisms. Parasitol Res 113:2407–2414. https://doi.org/10.1007/s00436-014-3932-7.
4. Whan L, Grant IR, Rowe MT. 2006. Interaction between Mycobacterium avium subsp. paratuberculosis and environmental protozoa. BMC Microbiol 6:63. https://doi.org/10.1186/1471-2180-6-63.
5. König L, Wentrup C, Schulz F, Wascher F, Escola S, Swanson MS, Buchrieser C, Horn M. 2019. Symbiont-mediated defense against Legionella pneumophila in amoebae. mBio 10:e00333-19. https://doi.org/10.1128/mBio.00333-19.
6. Rayamajhee B, Subedi D, Peguda HK, Willcox MD, Henriquez FL, Carnt N. 2021. A systematic review of intracellular microorganisms within Acanthamoeba to understand potential impact for infection. Pathogens 10:225. https://doi.org/10.3390/pathogens10020225.
7. Clarke M, Lohan AJ, Liu B, Lagkouvardos I, Roy S, Zafar N, Bertelli C, Schilde C, Kianianmomeni A, Bürglin TR, Frech C, Turcotte B, Kopec KO, Synnott JM, Choo C, Paponov I, Finkler A, Heng Tan CS, Hutchins AP, Weinmeier T, Rattei T, Chu JSC, Gimenez G, Irimia M, Rigden DJ, Fitzpatrick DA, Lorenzo-Morales J, Bateman A, Chiu C-H, Tang P, Hegemann P, Fromm H, Raoult D, Greub G, Miranda-Saavedra D, Chen N, Nash P, Ginger ML, Horn M, Schaap P, Caler L, Loftus BJ. 2013. Genome of Acanthamoeba castellanii highlights extensive lateral gene transfer and early evolution of tyrosine kinase signaling. Genome Biol 14:R11–R15. https://doi.org/10.1186/gb-2013-14-2-r11.
8. Wang Z, Wu M. 2017. Comparative genomic analysis of Acanthamoeba endosymbionts highlights the role of amoebae as a "melting pot" shaping the Rickettsiales evolution. Genome Biol Evol 9:3214–3224. https://doi.org/10.1093/gbe/evx246.
9. Cirillo JD, Cirillo SL, Yan L, Bermudez LE, Falkow S, Tompkins LS. 1999. Intracellular growth in Acanthamoeba castellanii affects monocyte entry mechanisms and enhances virulence of Legionella pneumophila. Infect Immun 67:4427–4434. https://doi.org/10.1128/IAI.67.9.4427-4434.1999.
10. Maumus F, Blanc G. 2016. Study of gene trafficking between Acanthamoeba and giant viruses suggests an undiscovered family of amoeba-infecting viruses. Genome Biol Evol 8:3351–3363. https://doi.org/10.1093/gbe/evw260.
11. Espinoza-Vergara G, Hoque MM, McDougald D, Noorian P. 2020. The impact of protozoan predation on the pathogenicity of Vibrio cholerae. Front Microbiol 11:17. https://doi.org/10.3389/fmicb.2020.00017.
12. Wang Y-J, Li S-C, Lin W-C, Huang F-C. 2021. Intracellular microbiome profiling of the Acanthamoeba clinical isolates from lens associated keratitis. Pathogens 10:266. https://doi.org/10.3390/pathogens10030266.
13. Garate M, Cao Z, Bateman E, Panjwani N. 2004. Cloning and characterization of a novel mannose-binding protein of Acanthamoeba. J Biol Chem 279:29849–29856. https://doi.org/10.1074/jbc.M402334200.
14. Yoo K-T, Jung S-Y. 2012. Effects of mannose on pathogenesis of Acanthamoeba castellanii. Korean J Parasitol 50:365–369. https://doi.org/10.3347/kjp.2012.50.4.365.
15. Jung S-Y. 2020. Inhibition of interactions between Acanthamoeba culbertsoni trophozoites and bacteria by antibodies to a mannose-binding protein. Biomedicine 40:198–202. https://doi.org/10.51248/v40i2.68.
16. Siddiqui R, Khan NA. 2012. Biology and pathogenesis of Acanthamoeba. Parasit Vectors 5:1–13. https://doi.org/10.1186/1756-3305-5-6.
17. Stehr-Green JK, Bailey TM, Visvesvara GS. 1989. The epidemiology of Acanthamoeba keratitis in the United States. Am J Ophthalmol 107:331–336. https://doi.org/10.1016/0002-9394(89)90654-5.
18. Qvarnstrom Y, Visvesvara GS, Sriram R, da Silva AJ. 2006. Multiplex real-time PCR assay for simultaneous detection of Acanthamoeba spp., Balamuthia mandrillaris, and Naegleria fowleri. J Clin Microbiol 44:3589–3595. https://doi.org/10.1128/JCM.00875-06.
19. Keshav BR, Basu S. 2012. Normal conjunctival flora and their antibiotic sensitivity in Omanis undergoing cataract surgery. Oman J Ophthalmol 5:16–18. https://doi.org/10.4103/0974-620X.94722.
20. Willcox MD. 2013. Characterization of the normal microbiota of the ocular surface. Exp Eye Res 117:99–105. https://doi.org/10.1016/j.exer.2013.06.003.
21. Graham JE, Moore JE, Jiru X, Moore JE, Goodall EA, Dooley JS, Hayes VE, Dartt DA, Downes CS, Moore TC. 2007. Ocular pathogen or commensal: a PCR-based study of surface bacterial flora in normal and dry eyes. Invest Ophthalmol Vis Sci 48:5616–5623. https://doi.org/10.1167/iovs.07-0588.
22. Grice EA, Kong HH, Renaud G, Young AC, Bouffard GG, Blakesley RW, Wolfsberg TG, Turner ML, Segre JA, NISC Comparative Sequencing Program. 2008. A diversity profile of the human skin microbiota. Genome Res 18:1043–1050. https://doi.org/10.1101/gr.075549.107.
23. Bonar E, Bukowski M, Chlebicka K, Madry A, Bereznicka A, Kosecka-Strojek M, Dubin G, Miedzobrodzki J, Mak P, Wladyka B. 2021. Human skin microbiota-friendly lysostaphin. Int J Biol Macromol 183:852–860. https://doi.org/10.1016/j.ijbiomac.2021.04.154.
24. Biswas K, Hoggard M, Jain R, Taylor MW, Douglas RG. 2015. The nasal microbiota in health and disease: variation within and between subjects. Front Microbiol 9:134. https://doi.org/10.3389/fmicb.2015.00134.
25. St Leger AJ, Desai JV, Drummond RA, Kugadas A, Almaghrabi F, Silver P, Raychaudhuri K, Gadjeva M, Iwakura Y, Lionakis MS, Caspi RR. 2017. An ocular commensal protects against corneal infection by driving an interleukin-17 response from mucosal γδ T cells. Immunity 47:148–158.e5. https://doi.org/10.1016/j.immuni.2017.06.014.
26. Yli-Pirilä T, Huttunen K, Nevalainen A, Seuri M, Hirvonen MR. 2007. Effects of co-culture of amoebae with indoor microbes on their cytotoxic and proinflammatory potential. Environ Toxicol 22:357–367. https://doi.org/10.1002/tox.20274.
27. Michel R, Hauröder-Philippczyk B, Müller K-D, Weishaar I. 1994. Acanthamoeba from human nasal mucosa infected with an obligate intracellular parasite. Eur J Protistol 30:104–110. https://doi.org/10.1016/S0932-4739(11)80203-8.

28. Allen PG, Dawidowicz EA. 1990. Phagocytosis in Acanthamoeba: I. A mannose receptor is responsible for the binding and phagocytosis of yeast. J Cell Physiol 145:508–513. https://doi.org/10.1002/jcp.1041450317.
29. Kim J-H, Matin A, Shin H-J, Park H, Yoo K-T, Yuan X-Z, Kim KS, Jung S-Y. 2012. Functional roles of mannose-binding protein in the adhesion, cytotoxicity and phagocytosis of Acanthamoeba castellanii. Exp Parasitol 132:287–292. https://doi.org/10.1016/j.exppara.2012.08.007.
30. Köhsler M, Leitsch D, Fürnkranz U, Duchêne M, Aspöck H, Walochnik J. 2008. Acanthamoeba strains lose their abilities to encyst synchronously upon prolonged axenic culture. Parasitol Res 102:1069–1072. https://doi.org/10.1007/s00436-008-0885-8.
31. Mazur T, Hadaś E. 1994. The effect of the passages of Acanthamoeba strains through mice tissue on their virulence and its biochemical markers. Parasitol Res 80:431–434. https://doi.org/10.1007/BF00932382.
32. Tsibidis GD, Burroughs NJ, Gaze W, Wellington EMH. 2011. Semi-automated Acanthamoeba polyphaga detection and computation of Salmonella typhimurium concentration in spatio-temporal images. Micron 42:911–920. https://doi.org/10.1016/j.micron.2011.06.010.
33. Yang Z, Cao Z, Panjwani N. 1997. Pathogenesis of Acanthamoeba keratitis: carbohydrate-mediated host-parasite interactions. Infect Immun 65:439–445. https://doi.org/10.1128/iai.65.2.439-445.1997.
34. Khan NA. 2006. Acanthamoeba: biology and increasing importance in human health. FEMS Microbiol Rev 30:564–595. https://doi.org/10.1111/j.1574-6976.2006.00023.x.
35. Marciano-Cabral F, Cabral G. 2003. Acanthamoeba spp. as agents of disease in humans. Clin Microbiol Rev 16:273–307. https://doi.org/10.1128/CMR.16.2.273-307.2003.
36. Niederkorn JY, Alizadeh H, Leher H, McCulley JP. 1999. The pathogenesis of Acanthamoeba keratitis. Microbes Infect 1:437–443. https://doi.org/10.1016/S1286-4579(99)80047-1.
37. Kong H-H, Kim T-H, Chung D-I. 2000. Purification and characterization of a secretory serine proteinase of Acanthamoeba healyi isolated from GAE. J Parasitol 86:12–17.2.0.CO;2. https://doi.org/10.1645/0022-3395(2000)086[0012:PACOAS]2.0.CO;2.
38. Alizadeh H, Pidherney MS, McCulley JP, Niederkorn JY. 1994. Apoptosis as a mechanism of cytolysis of tumor cells by a pathogenic free-living amoeba. Infect Immun 62:1298–1303. https://doi.org/10.1128/iai.62.4.1298-1303.1994.
39. Avery SV, Harwood JL, Lloyd D. 1995. Quantification and characterization of phagocytosis in the soil amoeba Acanthamoeba castellanii by flow cytometry. Appl Environ Microbiol 61:1124–1132. https://doi.org/10.1128/aem.61.3.1124-1132.1995.
40. Mantelli F, Mauris J, Argüeso P. 2013. The ocular surface epithelial barrier and other mechanisms of mucosal protection: from allergy to infectious diseases. Curr Opin Allergy Clin Immunol 13:563–568. https://doi.org/10.1097/ACI.0b013e3283645899.
41. Mayhew TM, Myklebust R, Whybrow A, Jenkins R. 1999. Epithelial integrity, cell death and cell loss in mammalian small intestine. Histol Histopathol 14:257–268. https://doi.org/10.14670/HH-14.257.
42. Shing B, Singh S, Podust LM, McKerrow JH, Debnath A. 2020. The antifungal drug isavuconazole is both amebicidal and cysticidal against Acanthamoeba castellanii. Antimicrob Agents Chemother 64:e02223-19. https://doi.org/10.1128/AAC.02223-19.
43. Chen C-H, Wang Y-J, Huang J-M, Huang F-C, Lin W-C. 2021. Inhibitory effect of host ocular microenvironmental factors on chlorhexidine digluconate activity. Antimicrob Agents Chemother 65:e02066-20. https://doi.org/10.1128/AAC.02066-20.
44. Bercovich-Kinori A, Israeli M, Chitlaru T, Cohen-Gihon I, Israeli O, Cohen O. 2020. Transcriptome sequencing data sets of human lung epithelial cells in the course of Francisella tularensis infection. Microbiol Resour Announc 9:e00991-20. https://doi.org/10.1128/MRA.00991-20.
45. Wang Y-J, Lin W-C, He M-S. 2021. The Acanthamoeba SBDS, a cytoskeleton-associated gene, is highly expressed during phagocytosis and encystation. J Microbiol Immunol Infect 54:482–489. https://doi.org/10.1016/j.jmii.2019.11.003.
46. Simmons PA, Tomlinson A, Seal DV. 1998. The role of Pseudomonas aeruginosa biofilm in the attachment of Acanthamoeba to four types of hydrogel contact lens materials. Optom Vis Sci 75:860–866. https://doi.org/10.1097/00006324-199812000-00007.
47. Huang J-M, Lin W-C, Li S-C, Shih M-H, Chan W-C, Shin J-W, Huang F-C. 2016. Comparative proteomic analysis of extracellular secreted proteins expressed by two pathogenic Acanthamoeba castellanii clinical isolates and a non-pathogenic ATCC strain. Exp Parasitol 166:60–67. https://doi.org/10.1016/j.exppara.2016.03.018.
48. Huang J-M, Liao C-C, Kuo C-C, Chen L-R, Huang LL, Shin J-W, Lin W-C. 2017. Pathogenic Acanthamoeba castellanii secretes the extracellular aminopeptidase M20/M25/M40 family protein to target cells for phagocytosis by disruption. Molecules 22:2263. https://doi.org/10.3390/molecules22122263.
49. Anwar A, Siddiqui R, Shah MR, Khan NA. 2018. Gold nanoparticle-conjugated cinnamic acid exhibits antiacanthamoebic and antibacterial properties. Antimicrob Agents Chemother 62:e00630-18. https://doi.org/10.1128/AAC.00630-18.
50. Park S-M, Lee H-A, Chu K-B, Quan F-S, Kim S-J, Moon E-K. 2020. Production of a polyclonal antibody against inosine-uridine preferring nucleoside hydrolase of Acanthamoeba castellanii and its access to diagnosis of Acanthamoeba keratitis. PLoS One 15:e0239867. https://doi.org/10.1371/journal.pone.0239867.
51. Mateos-Pérez JM, Pascau J. 2013. Image processing with ImageJ. Packt Publishing Ltd., Birmingham, UK.
52. Cariello AJ, Souza GFPd, Lowen MS, Oliveira MGd, Höfling-Lima AL. 2013. Assessment of ocular surface toxicity after topical instillation of nitric oxide donors. Arq Bras Oftalmol 76:38–41. https://doi.org/10.1590/s0004-27492013000100011.
53. Omaña-Molina M, González-Robles A, Iliana Salazar-Villatoro L, Lorenzo-Morales J, Cristóbal-Ramos AR, Hernández-Ramírez VI, Talamás-Rohana P, Méndez Cruz AR, Martínez-Palomo A. 2013. Reevaluating the role of Acanthamoeba proteases in tissue invasion: observation of cytopathogenic mechanisms on MDCK cell monolayers and hamster corneal cells. Biomed Res Int 2013:461329. https://doi.org/10.1155/2013/461329.
54. Ren M, Wu X. 2010. Evaluation of three different methods to establish animal models of Acanthamoeba keratitis. Yonsei Med J 51:121–127. https://doi.org/10.3349/ymj.2010.51.1.121.